Comparison Between ^{18}F-Florapronol and ^{18}F-Florbetaben Imaging in Patients With Cognitive Impairment

Kyoungwon Baik[a*]
Seun Jeon[a,b*]
Mincheol Park[a,c]
Young-gun Lee[a]
Phil Hyu Lee[a]
Young H. Sohn[a]
Byoung Seok Ye[a]

[a]Department of Neurology,
Yonsei University College of Medicine,
Seoul, Korea
[b]Brain Research Institute,
Department of Neurosurgery,
Yonsei University College of Medicine,
Seoul, Korea
[c]Department of Neurology,
Chung-Ang University
College of Medicine and
Graduate School of Medicine,
Gwangmyeong Hospital,
Gwangmyeong, Korea

Background and Purpose To determine the imaging characteristics and cutoff value of ^{18}F-florapronol (FC119S) quantitative analysis for detecting β-amyloid positivity and Alzheimer's disease (AD), we compared the findings of FC119S and ^{18}F-florbetaben (FBB) positron-emission tomography (PET) in patients with cognitive impairment.

Methods We prospectively enrolled 35 patients with cognitive impairment who underwent FBB-PET, FC119S-PET, and brain magnetic resonance imaging. We measured global and vertex-wise standardized uptake value ratios (SUVRs) using a surface-based method with the cerebellar gray matter as reference. Optimal global FC119S SUVR cutoffs were determined using receiver operating characteristic curves for β-amyloid positivity based on the global FBB SUVR of 1.478 and presence of AD, respectively. We evaluated the global and vertex-wise SUVR correlations between the two tracers. In addition, we performed correlation analysis for global or vertex-wise SUVR of each tracer with the vertex-wise cortical thicknesses.

Results The optimal global FC119S SUVR cutoff value was 1.385 both for detecting β-amyloid positivity and for detecting AD. Based on the global SUVR cutoff value of each tracer, 32 (91.4%) patients had concordant β-amyloid positivity. The SUVRs of FC119S and FBB had strong global ($r=0.72$) and vertex-wise ($r>0.7$) correlations in the overall cortices, except for the parietal and temporal cortices ($0.4<r<0.7$). The FC119S SUVR had significant negative vertex-wise correlations with cortical thicknesses in the posterior cingulate, anterior cingulate, parietal, posterior temporal, and occipital cortices.

Conclusions Quantitative FC119S-PET analysis provided reliable information for detecting β-amyloid deposition and the presence of AD.

Keywords amyloid-β; ^{18}F-florbetaben; ^{18}F-florapronol; positron emission tomography.

Correspondence
Byoung Seok Ye, MD, PhD
Department of Neurology,
Yonsei University College of Medicine,
50-1 Yonsei-ro, Seodaemun-gu,
Seoul 03722, Korea
Tel +82-2-2228-1609
Fax +82-2-393-0705
E-mail romel79@gmail.com

*These authors contributed equally to this work.

INTRODUCTION

Alzheimer's disease (AD) is the most common cause of dementia. Although a definite diagnosis of AD is possible at autopsy by using the cardinal pathological findings of β-amyloid plaques and neurofibrillary tangles,[1] the pathological process underlying AD could be detected by in vivo AD biomarkers for cerebral β-amyloid[2] and tau deposition.[3,4] To increase the accuracy of AD diagnosis, these biomarkers have been included in the research criteria for the diagnosis of AD.[5]

β-amyloid deposition is the most important and earliest detectable change in AD.[6,7] Several positron-emission tomography (PET) tracers have been developed to detect cerebral β-amyloid deposition. ^{11}C-Pittsburgh Compound-B (PiB) was the first developed β-amyloid-selective tracer,[8] which binds to fibrillar β-amyloid in neuritic plaques and other β-amyloid-containing lesions, including diffuse plaques and cerebral amyloid angiopathy.[9,10] To overcome the 20-min radioactive decay half-life that prevents its widespread clinical use, ^{18}F-

labeled tracers have been developed that have a longer half-life of 110 min.[11] Three ^{18}F-labeled tracers have received approval from the Food and Drug Administration and European Medicines Agency for clinical use and are widely used around the world: flutemetamol (Vizamyl, General Electric Healthcare, Milwaukee, MI, USA), florbetapir (Amyvid, Eli Lilly, Indianapolis, IN, USA), and ^{18}F-florbetaben (FBB; Neuraceq, Piramal, Mumbai, India).[11]

While ^{18}F-labeled tracers are suitable for clinical application, they still have some limitations. They bind nonspecifically to white matter, which reduces the signal background ratio. In addition, some widely used ^{18}F-labeled tracers require long waiting times after intravenous tracer administration prior to PET imaging, such as 90−110 min for the FBB tracer[12] and 90 min for the flutemetamol tracer,[13] making them inconvenient for clinical use. Therefore, there is a need to develop a tracer that has a shorter waiting time and exhibits reduced nonspecific binding.

A new ^{18}F-labeled amyloid tracer, ^{18}F-florapronol (FC119S), was developed in South Korea and obtained New Drug Application approval in 2018. It requires a relatively short waiting time after intravenous tracer administration (30−60 min). Previous studies have demonstrated the preclinical[14] and clinical relevance of FC119S in detecting β-amyloid deposition;[15] however, the imaging characteristics and cutoff value of quantitative analysis have not been clearly elucidated. In the present study, we compared the imaging characteristics of FC119S-PET and FBB-PET in patients with cognitive impairment. Based on the previously reported cutoff value for β-amyloid positivity on FBB-PET,[12] we aimed to determine the cutoff of quantitative FC119S analysis for detecting β-amyloid deposition.

METHODS

Participants
Thirty-nine patients with cognitive dysfunction whose β-amyloid statuses were determined using FBB-PET were consecutively recruited from November 2019 to January 2021. All patients underwent neurological examinations and neuropsychological tests, including the Korean version of the Mini Mental State Examination (K-MMSE), 3.0-T magnetic resonance imaging (MRI), ^{18}F-fluorodeoxyglucose (FDG)-PET, and FC119S-PET. K-MMSE was performed each time FC119S-PET and FBB-PET were performed. Based on a previously reported cutoff value for the quantitative analysis of FBB-PET,[12] a global FBB standardized uptake value ratio (SUVR) >1.478 was considered positive.

Fifteen patients had AD. All patients with AD dementia fulfilled the criteria for probable AD dementia with high lev-els of biomarker evidence;[16] all patients with mild cognitive impairment (MCI) due to AD met the criteria for a MCI due to AD-high likelihood according to the workgroups guidelines of the National Institute on Aging and Alzheimer's Association.[17] Patients with AD had memory problems as their chief complaint, and they showed entorhinal hypometabolism on FDG-PET[18] and a positive FBB-PET scan. Patients with positive FBB-PET scan but without memory problems or entorhinal hypometabolism were considered to have β-amyloid positivity but not AD. The final diagnosis of participant was made at the time of the final visit.

This study was approved by the Yonsei University Severance Hospital Institutional Review Board (IRB No. 4-2019-0865). Informed consent was obtained from all participants in the study.

Acquisition of MRI and PET data
Participants were scanned using a 3.0-T MRI scanner (Philips Achieva, Philips Medical Systems, Best, the Netherlands) with a SENSE head coil (SENSE factor=2). T1-weighted MRI data were obtained using a 3D T1-weighted turbo field echo sequence with the following parameters: axial acquisition matrix, 224×224; reconstructed matrix, 256×256 with 170 slices; voxel size, 0.859×0.859×1 mm³; field of view, 220 mm; echo time, 4.6 ms; repetition time, 9.8 ms; and flip angle, 8°.

FBB-PET and FC119S-PET data were acquired using a Discovery 600 scanner (General Electric Healthcare; Milwaukee, MI, USA). The FBB-PET images were acquired 90 min after FBB administration at 300 MBq (8 mCi) for 20 min. FC119S-PET images were acquired 30 min after FC119S administration at 370 MBq (10 mCi) for 30 min. PET images were acquired in a 256×256 matrix and were reconstructed using an ordered-subsets expectation-maximization algorithm in an isometric 0.98-mm voxel size.

Surface reconstruction and cortical thickness measurement
We applied the CIVET pipeline (http://mcin.ca/civet) to reconstruct cortical surfaces. The T1-weighted image of each participant was corrected for intensity inhomogeneities and linearly registered to the Alzheimer's Disease Neuroimaging Initiative−Montreal Neurological Institute atlas.[19] The image was then tissue-classified, and the inner and outer cortical surfaces were extracted, which yielded 40,962 vertex points per hemisphere.[20] Surfaces were registered to an unbiased group template by matching the sulcal folding pattern to obtain vertex correspondence between individuals. The cortical thickness was calculated as the distance Laplacian between the linked vertices of the inner and outer surfaces after transforming the surfaces back to the individual native space.

The measured cortical thickness was smoothed using a surface-based diffusion smoothing kernel (full width at half maximum of 30 mm).

PET image processing

Both FC119S-PET and FBB-PET images were linearly coregistered to the individual T1-weighted MRI scans at the corresponding time point using rigid body transformations. The reconstructed cortical surfaces and classified tissues from the CIVET pipeline were then linearly registered onto PET images by applying inverse-transform matrices. Partial volume correction was performed within the gray- and white-matter regions using iterative deconvolution using a surface-based anatomically constructed filtering method that represented the volume between the inner and outer surfaces as a spatial constraint to the PET signal.[21] The corrected PET images were normalized to the cerebellar gray-matter reference region to obtain SUVRs. The SUVR signal intensities were sampled at 50% of the distance from the inner to the outer surface to minimize partial-volume contamination. Measured signals were spatially blurred using a surface-based diffusion smoothing kernel with a full width at half maximum of 20 mm.

Based on the Desikan-Killiany-Tourville surface parcellation atlas, we expressed the global SUVR as the cortical volume-weighted average of the following cortical regions of interest (ROIs): frontal, anterior/posterior cingulate, parietal, and lateral temporal cortices. These ROIs were similar to those in previous studies that used FBB-PET to measure β-amyloid deposition, but we excluded the occipital ROI in our study because it showed a low β-amyloid load in AD-related changes.[22]

Quality assurance

Results from the image processing stages were visually inspected by three researchers (K.B., S.J., and B.S.Y.) who were blinded to the participant information. We excluded four participants due to MRI artifacts and image processing errors during the tissue classification and volume registration stages. The final analysis included 35 participants.

Statistical analysis

Statistical analyses were performed using the Statistical Package for the Social Sciences (version 26.0, IBM Corp., Armonk, NY, USA) for demographic and clinical variables, and SurfStat toolbox (http://www.math.mcgill.ca/keith/surfstat) for vertex-based statistics. The diagnostic accuracy of FC119S in detecting β-amyloid positivity based on quantitative analysis of FBB and the presence of AD was evaluated using receiver operating characteristic curve analysis and the area under the curve. Youden's index was used to determine the optimal cutoff for FC119S.[23] To determine the correlation between global β-amyloid burden measured on each tracer and general cognition, a partial correlation analysis was performed between the K-MMSE score and global SUVRs of each tracer after controlling for age, sex, and years of education. To determine the correlations between global β-amyloid burden measured using each tracer, a partial correlation analysis was performed after controlling for the above covariates and the time interval between acquiring the FC119S-PET and FBB-PET data.

The vertex-wise correlation between the cortical retentions of FBB and FC119S was evaluated using general linear models (GLMs). The effect of global β-amyloid burden on regional cortical thickness was determined by applying GLMs to the vertex-wise cortical thickness using the global SUVRs of each tracer as the predictors. To find the localized correlation between β-amyloid burden and cortical thickness, GLMs for vertex-wise cortical thickness were performed using each tracer's SUVRs at the same vertex as the predictor. All vertex-wise analyses were controlled for age, sex, years of education, intracranial volume, and the time interval between the acquisition of two scans. We used the false discovery rate (FDR) method to correct for multiple comparisons across the 81,924 cortical vertices, with FDR-corrected $p < 0.05$ considered significant. We displayed vertex-wise statistical outcomes on a standard cortical surface according to neurological convention.

RESULTS

Demographics and clinical characteristics

The demographic and clinical characteristics of participants are presented in Table 1. The study finally included 35 participants, including 9 males. The mean age of all participants was 78.57±7.10 years (mean±standard deviation) and 76.11± 7.21 years at the times of the FC119s-PET and FBB-PET scans, respectively. The interval between the two PET scans was 2.57±1.45 years. AD was diagnosed in 12 patients. All 23 participants without AD were diagnosed as dementia with Lewy bodies (DLB). The K-MMSE scores of all participants were 19.03±7.30 and 21.09±5.85 at the times of the FC119S-PET and FBB-PET scans, respectively. The mean global SUVRs for FC119S and FBB were 1.40 and 1.46, respectively. Individual uptake maps for FC119S and FBB are presented in Supplementary Fig. 1 (in the online-only Data Supplement).

FC119S SUVR cutoff for predicting FBB positivity and AD

The mean global SUVR of participants with positive FBB-

Table 1. Demographics and clinical characteristics (*n*=35)

Characteristic	Value
Age at FC119S-PET scan, years	78.57±7.10
Age at FBB-PET scan, years	76.11±7.21
Sex, male	9 (25.70)
Education, years	8.37±4.69
Diagnosis	
AD	12 (34.29)
Non-AD	23 (65.71)
K-MMSE score at time of FC119-PET scan	19.03±7.29
K-MMSE score at time of FBB-PET scan	21.09±5.85
FC119S	
Global SUVR	1.396±0.198
Frontal SUVR	1.357±0.157
Temporal SUVR	1.485±0.261
Parietal SUVR	1.347±0.198
Occipital SUVR	1.381±0.224
FBB	
Global SUVR	1.456±0.309
Frontal SUVR	1.439±0.296
Temporal SUVR	1.406±0.243
Parietal SUVR	1.456±0.292
Occipital SUVR	1.478±0.233

Data are expressed as mean±standard deviation or *n* (%) values.
AD, Alzheimer's disease; FBB, ^{18}F-florbetaben; FC119S, ^{18}F-florapronol; K-MMSE, Korean version of the Mini Mental State Examination; PET, positron-emission tomography; SUVR, standardized uptake value ratio.

PET was 1.831 for FBB-PET and 1.554 for FC119S-PET. The mean global SUVR of participants with negative FBB-PET was 1.284 for FBB-PET and 1.323 for FC119S-PET. The mean global SUVR of participants with AD was 1.796 for FBB-PET and 1.578 for FC119S-PET. The mean global SUVR of participants without AD was 1.278 for FBB-PET and 1.301 for FC119S-PET. The cutoff point of global FC119S SUVR based on Youden's index for predicting FBB positivity was 1.385 with a sensitivity of 90.9% and specificity of 91.7%. The cutoff point of global FC119S SUVR for predicting the presence of AD was 1.385 with a sensitivity of 91.7% and specificity of 95.7% (Fig. 1).

Concordance rate for SUVR cutoff categorization between FBB and FC119S

The concordance rate between FC119S and FBB was 91.4% (32/35) for SUVR cutoff categorization. The correlation coefficient between FC119S and FBB global SUVR was 0.71 (*p*< 0.001) (Fig. 2). Three participants presented intertracer discordance: participants A and B were positive for β-amyloid on FC119S-PET scan but negative on FBB-PET scan (Fig. 3A and B), while participant C was positive on FBB-PET scan but negative on FC119S-PET scan (Fig. 3C). Participant A

was a female patient aged 69 years (at the time of the FC119S-PET scan) and a heterozygous APOE4 carrier. Her chief complaint was difficulty in word finding. She exhibited memory, naming, and attentional deficits in a neuropsychological test and motor parkinsonism in a neurological examination. Based on decreased striatal dopamine transporter (DAT) uptake in DAT-PET, we diagnosed her as probable DLB based on the 2017 revised criteria for DLB.[24] The FC119S-PET scan was performed 0.5 years before the FBB-PET scan. Her global SUVR was 1.79 for FC119S and 1.38 for FBB, but her regional FBB SUVRs in the occipital and parietal regions were higher than 1.478.

Participant B was a female patient aged 63 years (at the time of the FC119S-PET scan) and a homozygous APOE4 carrier. The FC119S-PET scan was performed 0.5 years before the FBB-PET scan. Her global SUVR was 1.84 for FC119S and 1.41 for FBB, but her regional FBB SUVRs in the bilateral frontal and precuneus cortices were higher than 1.478. She was considered to have AD due to slowly progressive memory loss, FDG hypometabolism in the bilateral entorhinal, temporal, and parietal cortices, and regionally high FBB SUVRs in the bilateral frontal and precuneus cortices, although her global FBB SUVR was lower than the cutoff value of 1.478. She also had motor parkinsonism, REM sleep behavior disorder, and decreased DAT uptake in the left posterior putamen. We diagnosed her with mixed dementia (AD with probable DLB).

Participant C was a female patient aged 82 years (at the time of the FC119S-PET scan) and a heterozygous APOE4 carrier. Her chief complaints were memory dysfunction, cognitive fluctuation, and visual hallucination. She exhibited motor parkinsonism and decreased DAT uptake in the posterior putamen. The FBB-PET scan was performed 1.60 years before the FC119S-PET scan. Her global SUVR was 1.70 for FBB and 1.27 for FC119S. We diagnosed her as mixed dementia (AD with probable DLB).

Vertex-wise correlation between FC119S and FBB

The average regional SUVRs for FC119S in the FC119S-positive (global FC119S SUVR >1.385) and FC119S-negative groups are displayed in Fig. 4A and B, respectively, and those for FBB are presented in Fig. 4C and D. The regional SUVR differences between the β-amyloid-positive and β-amyloid-negative groups based on each tracer are displayed in Fig. 4E and F, respectively. The differences in regional SUVRs between β-amyloid-positive and β-amyloid-negative groups based on FBB-PET were prominent in the parietal and frontal cortices, while those based on FC119S-PET were prominent in the bilateral temporal cortices (but more on the left side). Vertex-wise correlations between the SUVRs of FC119S
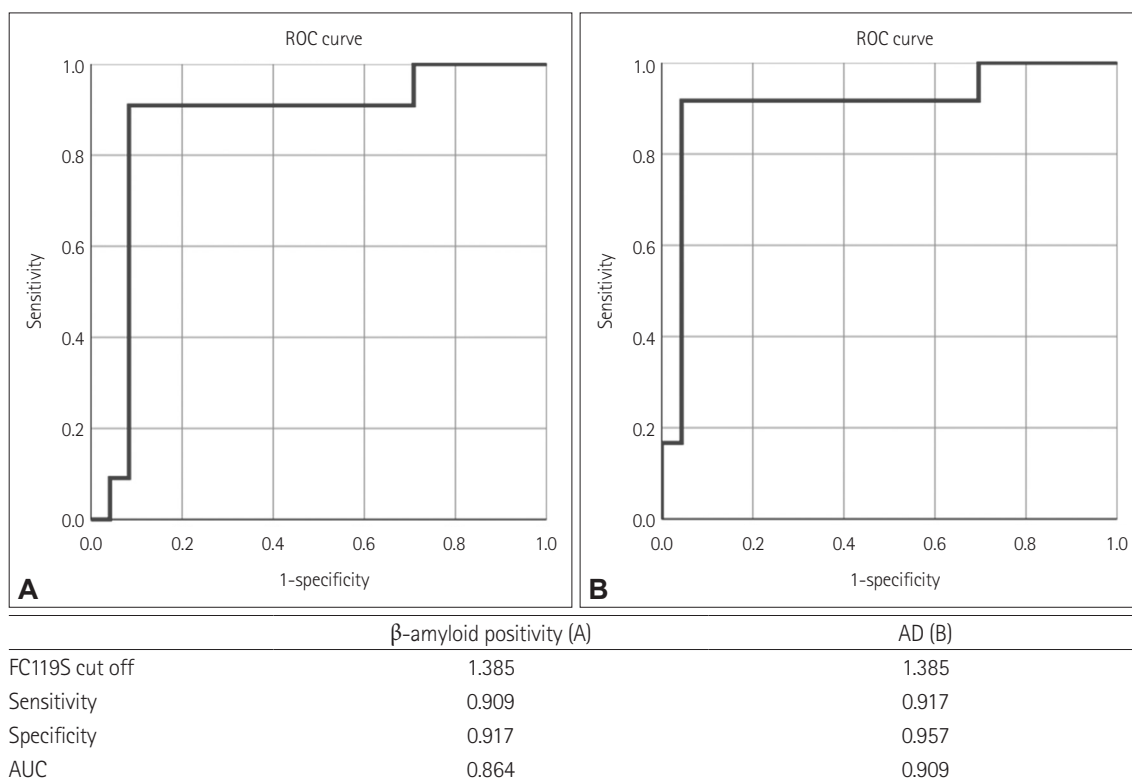
	β-amyloid positivity (A)	AD (B)
FC119S cut off	1.385	1.385
Sensitivity	0.909	0.917
Specificity	0.917	0.957
AUC	0.864	0.909

Fig. 1. ROC curves predicting β-amyloid positivity based on FBB-PET (cutoff value=1.478) (A) and presence of AD (B) based on the global FC119S SUVR. AD, Alzheimer's disease; AUC, area under the curve; FBB, ^{18}F-florbetaben; FC119S, ^{18}F-florapronol; PET, positron-emission tomography; ROC, receiver operating characteristics; SUVR, standardized uptake value ratio.
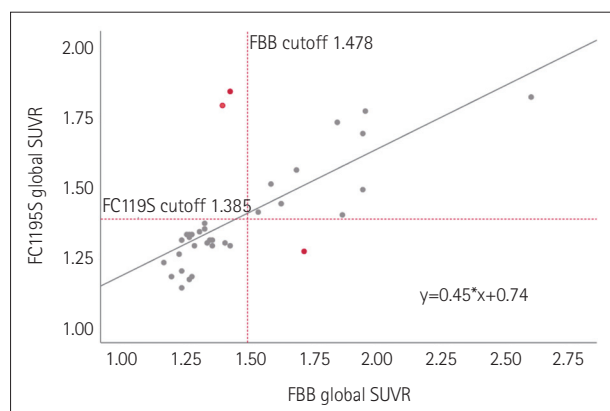
Fig. 2. Scatter plot of the relationship between the global SUVRs of FBB and FC119S. Red dots are participants with intertracer discordance between FC119S and FBB. FBB, ^{18}F-florbetaben; FC119S, ^{18}F-florapronol; SUVR, standardized uptake value ratio.

and FBB were strong in most brain regions, but moderate in the bilateral temporal and parietal cortices (Fig. 4G).

Correlation between cortical thickness and FC119S and FBB
Neither the global SUVR of FC119S nor that of FBB was associated with regional cortical thickness (Fig. 5A and B).

However, FC119S had significant vertex-wise correlations with cortical thickness in the cingulate, parietal, and occipital cortices (Fig. 5C), whereas FBB did not (Fig. 5D). Higher regional FC119S SUVRs in the cingulate and parietal cortices were associated with cortical thinning in those brain regions.

Correlation between global SUVR and K-MMSE score
Higher global SUVR for FC119S was associated with lower K-MMSE score (r=-0.665, p<0.001); there was no similar relationship between global SUVR for FBB and K-MMSE score (r=-0.224, p=0.227).

DISCUSSION

This study compared the imaging features of FC119S-PET and FBB-PET scans in patients with cognitive impairment. Our major findings were as follows: First, the cutoff value of global FC119S SUVR for determining the presence of significant β-amyloid deposition based on the previously reported global FBB SUVR cutoff value was 1.385, which was identical to that for the presence of AD. With the defined cutoff values, the two tracers had a strong global correlation and
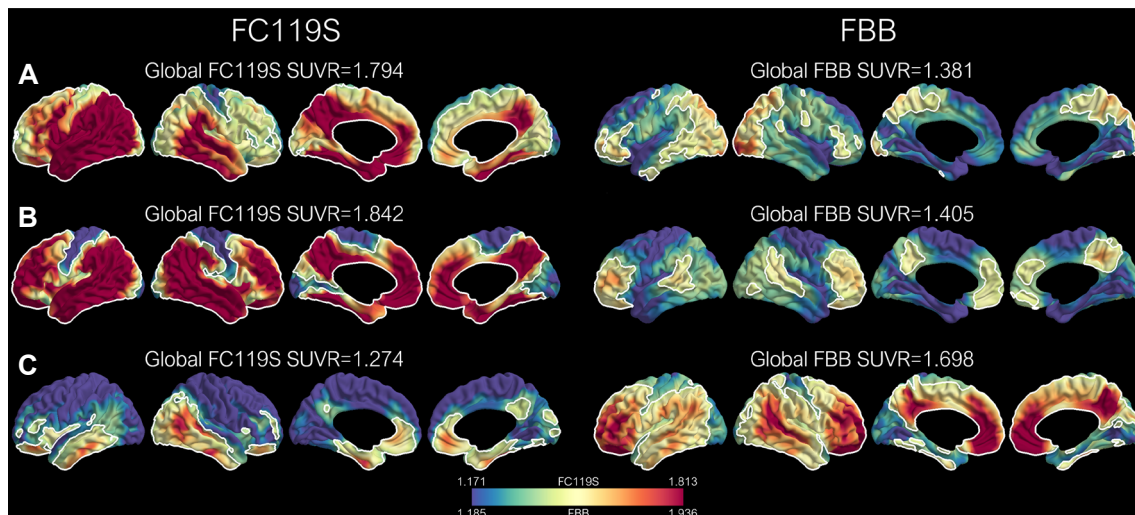
Fig. 3. Vertex-wise SUVR values in the two patients with FC119S-positive but FBB-negative scans (participants A and B), and the patient with FC119S-negative but FBB-positive scans (participant C). The red-colored numbers are the time intervals between the FC119S-PET and FBB-PET scans. The time interval was calculated as follows: (acquisition time of FC119S-PET)-(acquisition time of FBB-PET). The color scale is displayed using the 5th to 95th percentiles of each tracer. FBB, ^{18}F-florbetaben; FC119S, ^{18}F-florapronol; PET, positron-emission tomography; SUVR, standardized uptake value ratio.

high concordance rate of 91.4%. Second, predominant FC119S accumulation in the temporal cortices and that of FBB in the parietal cortices led to moderate correlations (0.4<r<0.7) between the tracers in the temporal and parietal cortices with strong regional correlations (r>0.7) in the other brain regions. Third, FC119S had a negative vertex-wise correlation with cortical thickness in the cingulate, parietal, and occipital cortices, whereas FBB did not. Moreover, higher global FC119S SUVRs were associated with lower K-MMSE scores. Taken together, our results suggest that FC119S has good efficacy in detecting cerebral β-amyloid deposition, and its vertex-wise correlation with cortical thickness and general cognition could be the unique characteristic of the FC119S tracer.

Based on previously reported cutoff values for surface-based quantitative analysis of FBB-PET scans, we found that a global FC119S SUVR cutoff value of 1.385 had the best classification accuracy for β-amyloid positivity and the presence of AD. This cutoff value was similar to that calculated from the previously reported regression equation of FC119S global SUVR=global PiB SUVR×0.41+0.72 that was derived from quantitative analyses of FC119S-PET and PiB-PET scans in healthy controls and patients clinically diagnosed with MCI and AD dementia.[15] The calculated global SUVR cutoff for FC119S was 1.335, which was derived from the previously reported global PiB SUVR cutoff of 1.5 for significant β-amyloid deposition.[25,26] Moreover, FC119S and FBB had a strong global correlation, and the classification of β-amyloid positivity based on FC119S had a high agreement rate of 91.4% compared with that based on FBB. Based

on a previous study that indicated excellent agreement between FC119S and PiB,[15] our results suggested that FC119S could be effective as a radiotracer for β-amyloid imaging.

FC119S accumulation was prominent in the temporal cortices, whereas FBB accumulation was prominent in the parietal cortices. These different regional preponderances resulted in moderate correlations (0.4<r<0.7) in the temporal and parietal cortices, and strong regional correlations (r>0.7) in other brain regions. These results were consistent with a previous study that found a prominent PiB SUVR in the parietal cortex and FC119S binding in the temporal cortex.[15] These regional differences may be related to the characteristics of the tracers, such as their affinity for the type of β-amyloid plaque. There are morphologically different amyloid plaques, including diffuse plaques and neuritic (or dense-cored) plaques,[27] and FBB binds to both of these types.[12,28] Considering the association between dystrophic neurites or tau pathology with neuritic plaques[1] and dense tau accumulation in the temporal cortex,[29] the regional preponderance of FC119S uptake may reflect that FC119S has a greater affinity for neuritic plaques than for diffuse plaques. Histopathological evidence is required from future studies to confirm this hypothesis.

The FC119S SUVRs had significantly negative vertex-wise correlations with cortical thickness, whereas the FBB SUVRs did not. Moreover, a higher global FC119S SUVR (but not that of FBB) was associated with a lower K-MMSE score. Considering that the tau burden is more strongly related to cortical thickness[30] and cognitive dysfunction[31] than is β-amyloid deposition, these results also supported that FC119S might have a greater affinity for neuritic plaques
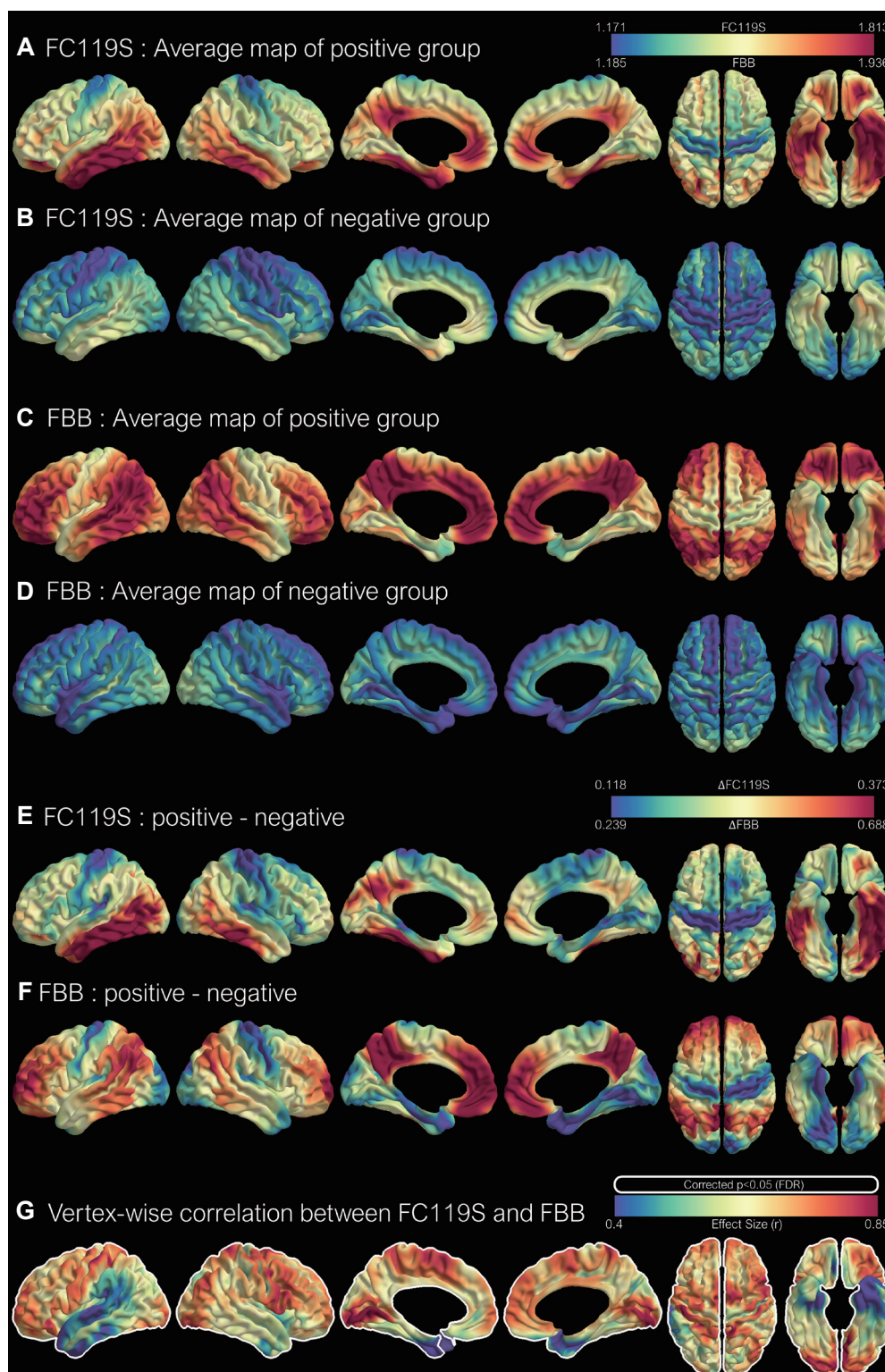
Fig. 4. Vertex-wise FC119S SUVR in FC119S-positive (global FC119S SUVR >1.385) (A) and FC119S-negative (B) groups. Vertex-wise FBB SUVR in FBB-positive (global FBB SUVR >1.478) (C) and FBB-negative (D) groups. Differences in vertex-wise FC119S SUVRs between FC119S-positive and FC119S-negative groups (E). Differences in vertex-wise FBB SUVRs between FBB-positive and FBB-negative groups (F). Vertex-wise correlation between the SUVRs of FC119S and FBB (G). Color scales indicate vertex-wise averaged SUVR uptakes (A–D), vertex-wise group differences in FC119S or FBB uptakes (E and F), and r values for the correlations (G). Color scales are displayed using the 5th to 95th percentiles of each tracer. The areas bounded by white lines indicate significantly correlated brain regions (FDR-corrected p<0.05). FBB, ^{18}F-florbetaben; FC119S, ^{18}F-florapronol; FDR, false discovery rate; SUVR, standardized uptake value ratio.
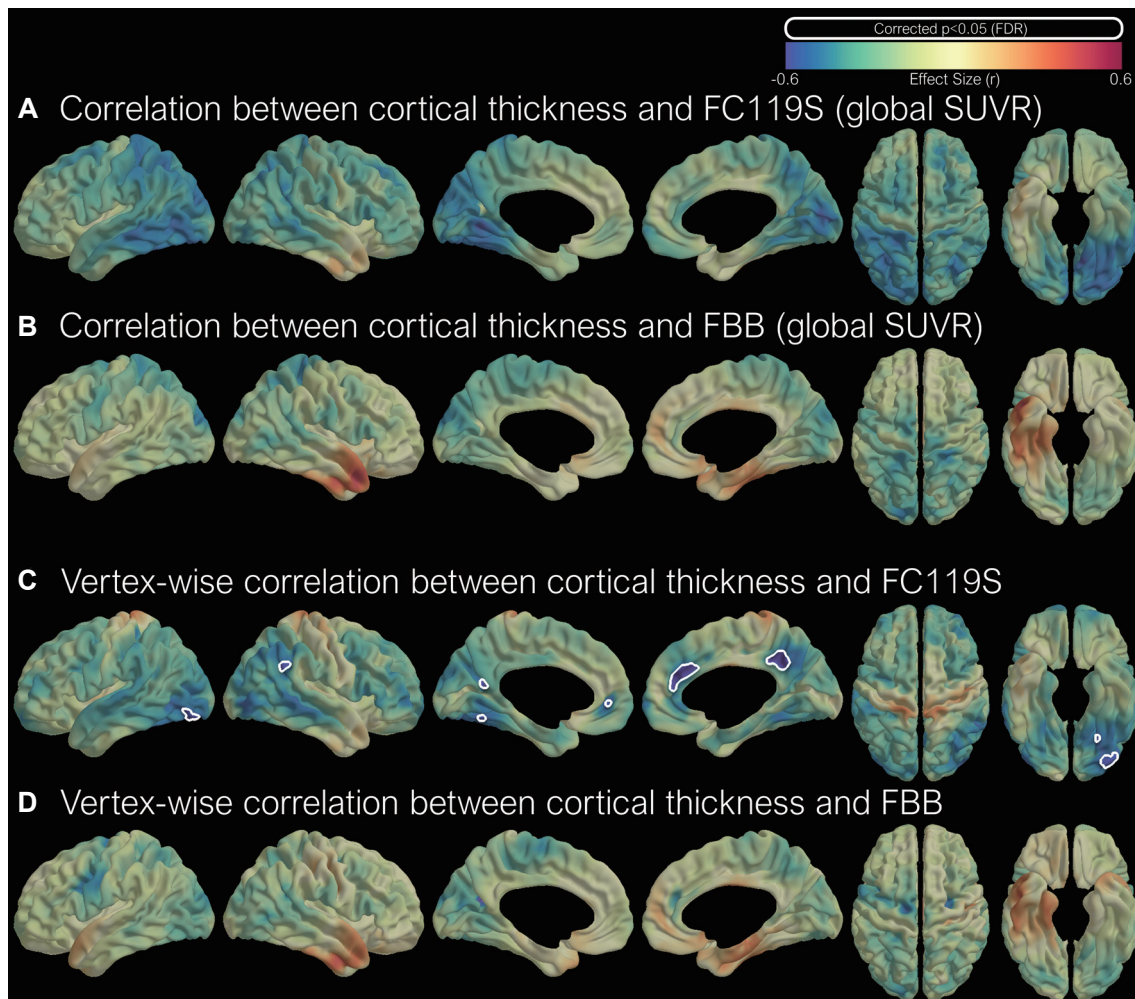
Fig. 5. Correlations of vertex-wise cortical thickness with the global SUVRs of FC119S SUVR (A) and FBB (B). Vertex-wise correlations of cortical thickness with the SUVRs of FC119S (C) and FBB (D). The color scale indicates the correlation coefficient in the statistical analysis. The areas bounded by the white line indicate brain regions significantly correlated with the predictors (FDR-corrected $p < 0.05$, FDR). FBB, ^{18}F–florbetaben; FC119S, ^{18}F–florapronol; FDR, false discovery rate; SUVR, standardized uptake value ratio.

than FBB. The cortical regions with significant vertex-wise correlations with FC119S SUVRs, including the posterior cingulate, anterior cingulate, parietal, posterior temporal, and occipital cortices, overlapped with the brain regions that had early and prominent tau deposition in patients with AD.[29] Based on the individual uptake map for FC119S in all participants in increasing order of global FC119S SUVR (Supplementary Fig. 1 in the online-only Data Supplement), we could identify the sequential order of topographical FC119S accumulation: it started from the entorhinal cortex, spread via the lateral temporal lobe, basal frontal lobe, and posterior cingulate cortex, and then reached the frontal, temporal, and inferior parietal lobes. This accumulation pattern was similar to the Braak neurofibrillary tangle stage in patients with AD.[32] Future studies involving tau imaging would be helpful to elucidate the relationship between FC119S and tau.

Three patients presented disagreement in β-amyloid positivity classification based on FC119S-PET and FBB-PET. Participants A and B presented β-amyloid positivity on FC119S-PET scan but β-amyloid negativity on FBB-PET, which was the opposite for participant C. Since all three of these patients had β-amyloid positivity in the first PET scan but β-amyloid negativity in the second PET scan, the discrepancies were not due to progression or worsening of β-amyloid accumulation. It was possible that participant C had diffuse plaques rather than neuritic plaques, which would explain the positive FBB-PET findings in the diffuse cortical regions including the cingulate cortex and the regional positivity in FC119S-PET in the temporal lobe including the transentorhinal cortex. It was also noteworthy that participants A and B were diagnosed with DLB and mixed dementia (AD with DLB), respectively. They both presented regional FBB positivity on quantitative FBB analysis. Previous studies found β-amyloid-

related[33] and β-amyloid-unrelated[34] tau accumulation in patients with DLB. Also, there could be an interplay between β-amyloid, tau, and α-synuclein.[35] β-amyloid deposition below the threshold and Lewy body pathologies in participants A and B could therefore have resulted in neuritic plaque accumulation and positive findings in FC119S-PET scans. Further molecular and immunohistochemical studies are required to confirm this hypothesis.

This study had several limitations. First, the time interval between FC119S and FBB scans was 2.57±1.45 years. We could not exclude the possibility that this time interval affected the identified cutoff value for FC119S. However, no subject was β-amyloid negative in the initial PET scan and β-amyloid positive in the subsequent scan, and so the discordance between the two tracers may not have been caused by the time between scans. Second, the SUVR cutoff of FC119S was determined based on FBB-PET positivity rather than on pathological confirmation. However, the cutoff value for the quantitative analysis of FBB-PET was obtained from the previous study with pathological confirmation of the diagnosis of AD.[12] Moreover, we performed comprehensive neurological and neuropsychological evaluations, and all patients underwent FDG-PET to obtain accurate diagnoses. Future studies that use both PET and autopsy data are needed to determine the cause of the discordance.

In summary, we demonstrated a strong global correlation between FC119S-PET and FBB-PET, and the excellent efficacy of detecting β-amyloid positivity and AD using FC119S. FC119S showed prominent accumulation of FC119S in the temporal cortex, correlation with general cognition, and vertex-wise correlation with cortical thickness, which might be the unique characteristics of the FC119S tracer. These results suggest that this new β-amyloid tracer has clinical implication for detecting not only β-amyloid deposition but also the presence of AD.

Supplementary Materials
The online-only Data Supplement is available with this article at https://doi.org/10.3988/jcn.2022.0207.

Availability of Data and Material
The datasets generated or analyzed during the study are available from the corresponding author on reasonable request.

ORCID iDs
Kyoungwon Baik   https://orcid.org/0000-0001-7215-375X
Seun Jeon   https://orcid.org/0000-0003-2817-3352
Mincheol Park   https://orcid.org/0000-0003-2714-7494
Young-gun Lee   https://orcid.org/0000-0003-0460-455X
Phil Hyu Lee   https://orcid.org/0000-0001-9931-8462
Young H. Sohn   https://orcid.org/0000-0001-6533-2610
Byoung Seok Ye   https://orcid.org/0000-0003-0187-8440

REFERENCES

1. DeTure MA, Dickson DW. The neuropathological diagnosis of Alzheimer's disease. *Mol Neurodegener* 2019;14:32.
2. Blennow K, Mattsson N, Schöll M, Hansson O, Zetterberg H. Amyloid biomarkers in Alzheimer's disease. *Trends Pharmacol Sci* 2015; 36:297-309.
3. Lowe VJ, Curran G, Fang P, Liesinger AM, Josephs KA, Parisi JE, et al. An autoradiographic evaluation of AV-1451 Tau PET in dementia. *Acta Neuropathol Commun* 2016;4:58.
4. Brier MR, Gordon B, Friedrichsen K, McCarthy J, Stern A, Christensen J, et al. Tau and Aβ imaging, CSF measures, and cognition in Alzheimer's disease. *Sci Transl Med* 2016;8:338ra366.
5. Jack CR Jr, Bennett DA, Blennow K, Carrillo MC, Dunn B, Haeberlein SB, et al. NIA-AA research framework: toward a biological definition of Alzheimer's disease. *Alzheimers Dement* 2018;14:535-562.
6. Hardy JA, Higgins GA. Alzheimer's disease: the amyloid cascade hypothesis. *Science* 1992;256:184-185.
7. Jack CR Jr, Knopman DS, Jagust WJ, Petersen RC, Weiner MW, Aisen PS, et al. Tracking pathophysiological processes in Alzheimer's disease: an updated hypothetical model of dynamic biomarkers. *Lancet Neurol* 2013;12:207-216.
8. Klunk WE, Engler H, Nordberg A, Wang Y, Blomqvist G, Holt DP, et al. Imaging brain amyloid in Alzheimer's disease with Pittsburgh compound-B. *Ann Neurol* 2004;55:306-319.
9. Driscoll I, Troncoso JC, Rudow G, Sojkova J, Pletnikova O, Zhou Y, et al. Correspondence between in vivo 11C-PiB-PET amyloid imaging and postmortem, region-matched assessment of plaques. *Acta Neuropathol* 2012;124:823-831.
10. Ikonomovic MD, Klunk WE, Abrahamson EE, Mathis CA, Price JC, Tsopelas ND, et al. Post-mortem correlates of in vivo PiB-PET amyloid imaging in a typical case of Alzheimer's disease. *Brain* 2008;131(Pt 6):1630-1645.
11. Morris E, Chalkidou A, Hammers A, Peacock J, Summers J, Keevil S. Diagnostic accuracy of 18F amyloid PET tracers for the diagnosis of Alzheimer's disease: a systematic review and meta-analysis. *Eur J Nucl Med Mol Imaging* 2016;43:374-385.
12. Sabri O, Sabbagh MN, Seibyl J, Barthel H, Akatsu H, Ouchi Y, et al. Florbetaben PET imaging to detect amyloid beta plaques in Alzheimer's disease: phase 3 study. *Alzheimers Dement* 2015;11:964-974.
13. Curtis C, Gamez JE, Singh U, Sadowsky CH, Villena T, Sabbagh MN, et al. Phase 3 trial of flutemetamol labeled with radioactive fluorine

18 imaging and neuritic plaque density. *JAMA Neurol* 2015;72:287-294.

14. Oh SJ, Lee HJ, Kang KJ, Han SJ, Lee YJ, Lee KC, et al. Early detection of Aβ deposition in the 5xFAD mouse by amyloid PET. *Contrast Media Mol Imaging* 2018;2018:5272014.

15. Byun BH, Kim BI, Park SY, Ko IO, Lee KC, Kim KM, et al. Head-to-head comparison of 11C-PiB and 18F-FC119S for Aβ imaging in healthy subjects, mild cognitive impairment patients, and Alzheimer's disease patients. *Medicine (Baltimore)* 2017;96:e6441.

16. McKhann GM, Knopman DS, Chertkow H, Hyman BT, Jack CR Jr, Kawas CH, et al. The diagnosis of dementia due to Alzheimer's disease: recommendations from the National Institute on Aging-Alzheimer's Association workgroups on diagnostic guidelines for Alzheimer's disease. *Alzheimers Dement* 2011;7:263-269.

17. Albert MS, DeKosky ST, Dickson D, Dubois B, Feldman HH, Fox NC, et al. The diagnosis of mild cognitive impairment due to Alzheimer's disease: recommendations from the National Institute on Aging-Alzheimer's Association workgroups on diagnostic guidelines for Alzheimer's disease. *Alzheimers Dement* 2011;7:270-279.

18. Ye BS, Lee S, Yoo H, Chung SJ, Lee YH, Choi Y, et al. Distinguishing between dementia with Lewy bodies and Alzheimer's disease using metabolic patterns. *Neurobiol Aging* 2020;87:11-17.

19. Fonov V, Coupe P, Eskildsen SF, Collins LD. Atrophy specific MRI brain template for Alzheimer's disease and mild cognitive impairment. Proceedings of the Alzheimer's Association International Conference; 2011 Jul 16-21; Paris, France: AAIC; 2011:S58.

20. Kim JS, Singh V, Lee JK, Lerch J, Ad-Dab'bagh Y, MacDonald D, et al. Automated 3-D extraction and evaluation of the inner and outer cortical surfaces using a Laplacian map and partial volume effect classification. *Neuroimage* 2005;27:210-221.

21. Funck T, Paquette C, Evans A, Thiel A. Surface-based partial-volume correction for high-resolution PET. *Neuroimage* 2014;102(Pt 2):674-687.

22. Lee YG, Jeon S, Yoo HS, Chung SJ, Lee SK, Lee PH, et al. Amyloid-β-related and unrelated cortical thinning in dementia with Lewy bodies. *Neurobiol Aging* 2018;72:32-39.

23. Youden WJ. Index for rating diagnostic tests. *Cancer* 1950;3:32-35.

24. McKeith IG, Boeve BF, Dickson DW, Halliday G, Taylor JP, Weintraub D, et al. Diagnosis and management of dementia with Lewy bodies: fourth consensus report of the DLB consortium. *Neurology* 2017;89:88-100.

25. Lee JH, Kim SH, Kim GH, Seo SW, Park HK, Oh SJ, et al. Identification of pure subcortical vascular dementia using 11C-Pittsburgh compound B. *Neurology* 2011;77:18-25.

26. Ye BS, Kim HJ, Kim YJ, Jung NY, Lee JS, Lee J, et al. Longitudinal outcomes of amyloid positive versus negative amnestic mild cognitive impairments: a three-year longitudinal study. *Sci Rep* 2018;8:5557.

27. Dickson TC, Vickers JC. The morphological phenotype of beta-amyloid plaques and associated neuritic changes in Alzheimer's disease. *Neuroscience* 2001;105:99-107.

28. Sabri O, Catafau A, Barthel H, Seibyl J, Ghetti B, Leverenz J, et al. Impact of morphologically distinct amyloid β (Aβ) deposits on 18F-florbetaben (FBB) PET scans. *J Nucl Med* 2015;56(supplement 3):195.

29. Cho H, Choi JY, Hwang MS, Kim YJ, Lee HM, Lee HS, et al. In vivo cortical spreading pattern of tau and amyloid in the Alzheimer disease spectrum. *Ann Neurol* 2016;80:247-258.

30. Harrison TM, Du R, Klencklen G, Baker SL, Jagust WJ. Distinct effects of beta-amyloid and tau on cortical thickness in cognitively healthy older adults. *Alzheimers Dement* 2021;17:1085-1096.

31. Ossenkoppele R, Smith R, Ohlsson T, Strandberg O, Mattsson N, Insel PS, et al. Associations between tau, Aβ, and cortical thickness with cognition in Alzheimer disease. *Neurology* 2019;92:e601-e612.

32. Braak H, Braak E. Neuropathological stageing of Alzheimer-related changes. *Acta Neuropathol* 1991;82:239-259.

33. Kantarci K, Lowe VJ, Boeve BF, Senjem ML, Tosakulwong N, Lesnick TG, et al. AV-1451 tau and β-amyloid positron emission tomography imaging in dementia with Lewy bodies. *Ann Neurol* 2017;81:58-67.

34. Gomperts SN, Locascio JJ, Makaretz SJ, Schultz A, Caso C, Vasdev N, et al. Tau positron emission tomographic imaging in the Lewy body diseases. *JAMA Neurol* 2016;73:1334-1341.

35. Obi K, Akiyama H, Kondo H, Shimomura Y, Hasegawa M, Iwatsubo T, et al. Relationship of phosphorylated alpha-synuclein and tau accumulation to Aβ deposition in the cerebral cortex of dementia with Lewy bodies. *Exp Neurol* 2008;210:409-420.